UCRL-CONF-225802

LAWRENCE
LIVERMORE
NATIONAL
LABORATORY

Laser Beam Propagation through Inertial Confinement Fusion Hohlraum Plasmas

D. H. Froula, L. Divol, N. B. Meezan, S. DIxit, P. Neumayer, J. D. Moody, B. B. Pollock, J. S. Ross, S. H. Glenzer

November 2, 2006

Disclaimer

Laser Beam Propagation through Inertial Confinement Fusion Hohlraum Plasmas

D. H. Froula,[*] L. Divol, N. B. Meezan, S. Dixit, P. Neumayer,

J. D. Moody, B. B. Pollock,[†] J. S. Ross, and S. H. Glenzer

L-399, Lawrence Livermore National Laboratory, P.O. Box 808, Livermore, CA 94551, USA

(Dated: October 26, 2006)

A study of the relevant laser-plasma interaction processes has been performed in long-scale length plasmas that emulate the plasma conditions in indirect drive inertial confinement fusion targets. Experiments in this high-temperature ($T_e = 3.5$ keV), dense ($n_e = 0.5-1 \times 10^{21} \text{cm}^{-3}$) hohlraum plasma have demonstrated that blue 351-nm laser beams produce less than 1% total backscatter resulting in transmission greater than 90% for ignition relevant laser intensities ($I < 2 \times 10^{15} W \text{cm}^{-2}$). The bulk plasma conditions have been independently characterized using Thomson scattering where the peak electron temperatures are shown to scale with the hohlraum heater beam energy in the range from 2 keV to 3.5 keV. This feature has allowed us to determine the thresholds for both backscattering and filamentation instabilities; the former measured with absolutely calibrated full aperture backscatter and near backscatter diagnostics and the latter with a transmitted beam diagnostics. Comparing the experimental results with detailed gain calculations for the onset of significant laser scattering processes shows that these results are relevant for the outer beams in ignition hohlraum experiments corresponding to a gain threshold for stimulated Brillouin scattering of 15. By increasing the gas fill density in these experiments further accesses inner beam ignition hohlraum conditions. In this case, stimulated Raman scattering dominates the backscattering processes. We show that scattering is small for gains smaller than 20, which can be achieved through proper choice of the laser beam intensity.

INTRODUCTION

Inertial confinement fusion (ICF) and high energy density physics experiments [1] with mega-joule class lasers require intense and energetic laser beams to propagate through large-scale length plasmas and to deposit their energy in the target for efficient production of soft or hard x rays. Radiation cavities, called hohlraums, are employed to confine the radiation and to efficiently produce thermal soft x-ray emission. In present indirect drive inertial confinement fusion designs, a fusion capsule is placed in the center of a hohlraum and the soft x rays from the walls are absorbed in the capsule ablator to implode and ignite the deuterium-tritium plasma. These hohlraums employed in ICF research use a low-Z cryogenic gas fill to prevent fast wall plasma blow off, which may impose asymmetric capsule implosion conditions. Consequently, the laser beams have to initially propagate through up to 1 cm of dense low-Z plasma before they deposit their energy in the hohlraum wall.

The physics of ignition hohlraums includes radiation production and confinement, and the laser-plasma interaction processes that determine laser beam propagation, scattering and absorption. Generally, predictive modeling of the laser-plasma interaction processes requires detailed understanding of instabilities including laser backscattering by Stimulated Brillouin Scattering (SBS) and Stimulated Raman Scattering (SRS), laser beam deflection, beam filamentation, and self focusing [2]. Moreover, a generally applicable quantitative model

will need to include the different hohlraum materials and the nonlinear evolution of the instabilities. The development and testing of such a capability is an ongoing research activity and is presently providing guidance on experiments that apply high laser intensities. However, for the design of ignition hohlraum targets at the National Ignition Facility (NIF) we have adopted the strategy to choose moderate laser intensities and beam smoothing conditions for which the gains of various laser-plasma instabilities are moderately small so that efficient laser beam propagation and high x-ray production may be expected.

In this study, we have determined, through experiments at the Omega laser facility [4], the plasma conditions and the range of gain values of laser-plasma instabilities that result in small backscattering and filamentation processes such as desired for ignition hohlraum plasmas. For this purpose, we have developed new high-temperature hohlraum targets that reach electron temperatures of up to $T_e = 4$ keV at a scale length of $1-2$ mm and electron densities of $n_e/n_{crit} = 0.06 - 0.12$. Here, $n_{crit} = 10^{22} \text{cm}^{-3}$ is the critical density for 351-nm laser light. For this study, CH-gas fills have been chosen emulating the plasma conditions in the hohlraum interior of present ignition hohlraum design .

The bulk plasma conditions are well characterized with Thomson scattering allowing us to determine the gain values for which laser backscattering and filamentation processes become important. A 4ω-probe laser has been focussed into the center of the hohlraum and the ion fea-

ture of the Thomson-scattered light spectrum was temporally resolved with a streaked spectrometer. Thus, the electron temperature, T_e, and the ion temperature, T_i, have been both measured accurately and simultaneously. We find $T_e/T_i \approx 3$ and T_e being determined by the hohlraum heater beam laser energy providing a temperature range of 2 keV$< T_e < 3.5$ keV in the present study. Since SBS and SRS gain values are sensitive to T_e as well as to T_e/T_i, Thomson scattering has allowed us to directly calculate the laser-plasma interaction instability gains for each shot.

The SBS reflectivity has been measured employing the absolutely calibrated full aperture backscatter and near backscatter diagnostics at Omega. These measurements are complemented by the transmitted beam diagnostics that measures the transmitted laser power, spectrum, and the laser beam spots. This complete suite of diagnostics allows us to determine the beam energetics by completely accounting for the scattered and absorbed laser power . Furthermore, the transmitted laser beam spot measurements detect beam spray due to filamentation and self-focussing effects .

Two conditions have been extensively studied that correspond to the plasma regimes encountered by the laser beams in the different cones in an ignition hohlraum. NIF has 4 cones of quads of beams that irradiate the hohlraum at 23°, 30°, 44°, and 50° to the hohlraum axis. Since the 44°, and 50° beams both primarily encounter hot ($T_e > 3$ keV) and moderately dense ($n_e/n_{crit} = 0.06$) plasmas conditions before irradiating the hohlraum walls they are referred to as outer beam. The 23°, 30° beams, on the other had, first propagate through similar conditions like the outer beams before they encounter denser ($n_e/n_{crit} \simeq 0.15$) moderately hot ($2.5 < T_e < 3.5$ keV) plasmas conditions. They are accordingly noted as inner beams.

For the outer beam emulator conditions, we find that SRS is negligibly small and the backscattering is dominated by SBS light. By increasing the electron temperature of the plasma from $T_e = 2$ keV to $T_e = 3.5$ keV we find for the highest relevant laser beam intensities of $I = 2 \times 10^{15} W \mathrm{cm}^{-2}$ that the SBS reflectivity drops to < 1 %. This correspond to a gains of $G_{SBS} < 15$.

For inner beam emulator plasma conditions with higher densities of $n_e/n_{crit} = 0.12$, we generally find that SRS dominates the backscattering and SBS is moderately small, but not negligible. The high electron densities occur in ignition hohlraums in close proximity to the fusion capsule where the inner beams interact with the ablator blow off plasmas. Optimizing the fusion capsule performance by choosing a hydrodynamic efficient ablators, for example beryllium compared to CH, will cause the electron density in this region of the hohlraum interior to be significantly larger than for the outer beams. Our experiments show that SRS can be controlled and reduced to small levels of < 5 % for laser beam intensities of

$I \simeq 4 \times 10^{14} W \mathrm{cm}^{-2}$. These results provide important guidance for future ignition experiments. It is planned to choose the inner laser beam spots so that the intensity will remain below this limit at the position in the hohlraum where they begin interacting with the high-density plasma.

Section   presents the experimental setup where the high-temperature hohlraum targets, the heater and interaction laser beam configurations, the suite of diagnostics, and radiation-hydrodynamics simulation results are presented. The laser backscatter measurements for the outer and inner beam hohlraum plasma emulator experiments are presented in Sec. . The paper concludes in Sec. .

EXPERIMENT

High Electron-temperature Targets

The experiments were performed with the Omega Laser Facility at the Laboratory for Laser Energetics [4]. The laser facility consists of 60 frequency tripled Nd:glass laser beams with approximately 500 J per beam of 351 nm (3ω) laser light on target. In these experiments, one of the 3ω f/6.7 beams (B30) is fully equipped with laser backscattering and transmission diagnostics that has been configured as an interaction beam with dedicated Continuous Phase Plates (CPP) , Smoothing by Spectral Dispersion (SSD), and appropriate delay with respect to the heater beams. A 2-mm long, 1.6-mm diameter gas-filled hohlraum has been aligned along the axis of the interaction beam so that the beam propagates through the heated hohlraum plasma (Fig. 1) interacting with a $\sim$ 2-mm long high temperature plasma. At the center of the hohlraum, laser beam intensities of up to $I \simeq 4 \times 10^{15} W \mathrm{cm}^{-2}$ have been achieved in the CPP-smoothed spot with a minimum vacuum diameter of 100 microns. The power averaged intensity of the interaction beam has been varied by changing the energy of the beam; $I_p = 8.5 \times 10^{12} E[J]$, where E is the incident laser beam energy ranging from 100 J to 400 J.

The hohlraums are heated with up to 37 3ω beams with total heater beam energy ranging from 8 kJ to 17 kJ in a 1 ns flat top laser pulse with 0.1 ns rising and falling edges. The heater beams penetrate the hohlraum at both ends through laser entrance holes with a diameter of 0.8 mm which are covered with 0.35 micron thick polyimide membranes to contain the gas fill. The choice of the initial hydro-carbon gas fill density allows us to vary the electron density in the interaction beam path for emulating outer or inner beam conditions.

The electron temperature along the interaction beam path is controlled by varying the heater beam energy from a maximum of 17 kJ; the plasma conditions along the interaction beam path have been measured using

Thomson scattering. These measurements have validated 2-dimensional HYDRA [5] radiation-hydrodynamic simulations that show a uniform 1.6-mm plasma with a peak electron temperature of 3.5 keV [3]. The laser-plasma interaction experiments are performed in this well-characterized uniform hohlraum plasma at homogeneous density before shock waves driven by heater laser beam ablation at the gold wall reach the hohlraum axis, t $\simeq$ 1.3ns (stagnation)[6].

Hydrodynamic modeling of the experiments have been performed in two dimensions using the code HYDRA [5] where the heat flux is determined by either a flux limited diffusion model or a nonlocal model . The primary difference between the nonlocal and flux limited models is the ability for the nonlocal model to inhibit the heat flux where there are large gradients while still allowing the fast electrons to carry away the heat. For example, in the presence of large temperature gradients, the flux limited model tends to either over estimate the heat flux (large flux limiter) artificially reducing the temperature gradient, or under estimate the heat flux (small flux limiter) therefore, preventing the surrounding plasma from getting hot. We find that both models indicate peak electron temperatures of order 3.5 keV in the 2 mm long flat density bulk plasma along the hohlraum axis, However, the nonlocal model shows larger temperature gradients resulting from the local laser beam heating that tends to reduce the calculated heat flux, therefore, increasing the temperature inside of the laser beams. The calculations indicate this heating around the laser entrance hole areas where several beams overlap. Such gradients have also been experimentally observed in previous Thomson-scattering measurements on the Nova laser facility [6]. However, the calculations of the bulk plasma conditions are insensitive to the choice of the heat transport modeling indicating our ability to correctly calculate the gain for laser-plasma interaction processes in these targets.

This new target platform together with recently commissioned suite of laser-plasma interaction diagnostics [7, 8] allows the access to high temperature, long scale length conditions not previously available using gasbag [9, 10], toroidal hohlraum [11, 12], or gas-filled hohlraum targets. Laser-plasma interaction thresholds are sensitive to the electron temperature and the length of the density plateau in a plasma; electron temperatures in open geometry gasbag plasmas with roughly the same plasma scale-lengths are significantly lower than in the present hohlraum targets because of factor of 10 larger energy density in hohlraums. Moreover, the capability to align the interaction beam along the hohlraum axis allowed us to reach significantly larger scale lengths than previous gas-filled hohlraum experiments with the added benefits of accurate Thomson scattering characterization and direct transmission measurements.
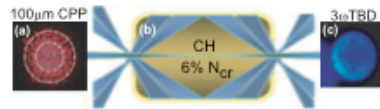

FIG. 1: A 3ω interaction beam smoothed with a CPP (a) and a maximum power averaged intensity of 4×10^{15} W-cm^{-2} is aligned along the axis of a gas-filled hohlraum (b) where 33 heater beams heat the CH gas to a maximum electron temperature of 3.5 keV. The electron temperature at the center of the hohlraum is measured using Thomson scattering where the total heater beam energy has been scaled from 8 kJ to 17 kJ. The transmitted power and near field beam profile indicates a transparent plasmas for $T_e > 3$ keV.

Thomson scattering

The plasma conditions in the center of the hohlraum have been measured temporally resolved with 4ω Thomson scattering. One of the 3ω beams (beam 25) has been de-tuned to produce 2ω light and directed to a dedicated port (P9) and subsequently doubled to provide a 4ω Thomson-scattering probe laser [7]. Typical 4ω probe beam energies of E=200 J with a flat 1 ns pulse duration have been employed with a small focal spot of 60 μm at the Thomson-scattering volume. The scattered light is imaged, at a scattering angle of $\theta = 101^o$, through a diagnostic window (500 μm×500 μm) cut in the side of the hohlraum wall. The hole is covered with a 0.26 micron thick polyimide window when a gas fill is employed. The scattering parameter is $\alpha = 1.4$ for plasma conditions of $T_e = 4$ keV and $n_e = 6 \times 10^{20}$ cm^{-3} where the scattering parameter α for our geometry is,

$$\alpha = 1 \times 10^{-10} \left(\frac{n_e[cm^{-3}]}{T_e[keV]} \right)^{1/2} \qquad (1)$$

In our experiment T_i/ZT_e is always smaller than the square of the scattering parameter ($\alpha^2 > T_i/ZT_e$), therefore, collective ion-acoustic modes are observed.

The wavelength shift of the ion-acoustic modes in the Thomson scattering spectrum are determined by the plasma conditions (primarily temperature), probe laser wavelength, λ_0 , and the scattering angle θ. Two features are observed corresponding to ion acoustic modes propagating and counter-propagating along the scattering vector **k** with k = $4\pi/\lambda_0\sin(\theta/2)$. In our conditions, the wavelength shift between the two ion acoustic peaks is of order $0.5 - 1$ nm.

To spectrally and temporally resolve the scattered light spectrum we fielded an achromatic collection system. The scattered light is collected and collimated by an $f/10$ achromatic lens with a 50 cm focal length. A blast shield with a coating to reject the scattered light from the 3ω heater beams has been implemented prior to the collection lens. A 7.5 cm focusing mirror with a 75 cm focal length images the scattered light onto the 150 μm slit of
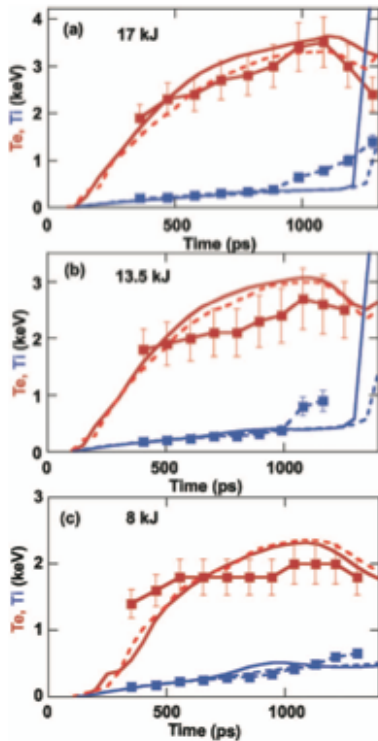
FIG. 2: The electron and ion temperature from Thomson scattering measurements at the center of the hohlraum is shown as function of time. The total heater beam energy has been varied from 8 kJ to 17 kJ indicating that the bulk plasmas conditions can be controlled up to electron temperatures like those expected in ignition hohlraums.

a 1-meter imaging spectrometer with a 3600 lines/mm grating. A high dynamic range streak camera is coupled to the spectrometer through a 200 μm temporal slit.

The Thomson-scattering volume (60 μm$\times$110 μm$\times$80 μm) is defined by the beam waist of the probe beam (60 μm) and the projection of the spectrally and temporally resolving slits into the plasma. The location of the scattering volume is known to the accuracy of the target alignment system which is better than 50 μm.

The scattered frequency spectrum provides a measure of the local particle flow velocity and the ion-acoustic sound speed that is directly related to the electron temperature. In our two-ion-species carbon-hydrogen plasmas, the relative amplitude of the light scattered from the two ion-acoustic modes allows an accurate determination of the ion temperature The results for the ion and electron temperature at the center of the hohlraum are shown in Fig. 2 for 8 kJ, 13.5 kJ, and 17 kJ heater beam energy into the hohlraum.

Transmitted Beam Diagnostics

The Transmitted Beam Diagnostics (TBD) measures the laser light transmitted through the target chamber center (TCC) within twice the original $f/6.7$ beam cone of the Omega beam 30 operated at 3ω . At 60 cm past TCC, a 25-cm-diameter uncoated fused silica focusing mirror, $f = 44$ cm, directs 4% of the transmitted light through a 10-cm diameter port on the target chamber. The focusing mirror is inserted through a Ten Inch diagnostics Manipulator port.

The beam propagates out of the target chamber onto a diagnostic table where the transmitted beam energy is directly measured using two calorimeters. One calorimeter measures the energy of the forward stimulated Brillouin scattering FSBS contribution and a second the forward stimulated Raman scattering FSRS . In addition, a small fraction of the light is picked-off to measure the full-aperture transmitted power, spectrum, and a near field image of the transmitted light. The FSBS and the FSRS measurement employ two spectrometers equipped with optical streak cameras.

While the total transmitted beam power is an important quantity to determine the energetics of the laser-plasmas interactions the near field measurements provide the transmitted focal spot and directly measure beam spray induced by scattering processes and filamentation. The latter employs two gated intensified 16 bit CCD cameras imaging twice the initial $f/6.7$ cone with two 105 mm $f/4.5$ achromatic 250650 nm lenses. This system is capable to resolve beam spray of 1 degree.

Backscattering diagnostics

Light scattered from the 3ω interaction beam is measured using a Full-Aperture Back Scattering station (FABS), a Near Backscattering Imager (NBI), and a Transmitted Beam Diagnostics (TBD). Light scattered back into the original beam f-cone is collected by FABS; both the SBS (350-352 nm) and the SRS (500-600 nm) spectrum and energy are independently measured. The FABS collects light that has been backscattered into the 30-cm focusing lens. The backscattered light is collimated by the lens and reflected by the last turning mirror. About 95% of the backscattered light is transmitted and picked off by a bare surface wedged optics.

The SRS and SBS light is separated by a wedged optics and filters. Two calorimeters measure the total SBS and SRS energy. The system is calibrated *in situ* at 351 nm using a low-energy laser shot that is reflected straight back into the FABS by an aluminum mirror before the focussing lens. Before the calorimeters a small fraction of the light is picked off into optical fibers and the SBS and SRS spectra are recorded using spectrometers equipped with optical streak cameras. The spectra were measured
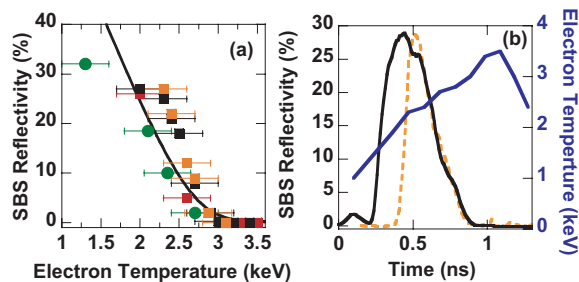
FIG. 3: (a) The SBS reflectivity is significantly reduced as the electron temperature is increased for an intensity of $I_p = 1.7 \times 10^{15}$ W cm^{-2}. The instantaneous reflectivities are obtained by time resolving the backscatter and varying the total heater beam energy from 8 kJ (circles) to 16 kJ (squares). Each point represents an average over 200 ps and each color corresponds to a separate shot. (b) By delaying the interaction beam by 200 ps (dashed orange line) the beam interacts primarily with hot plasma thus reducing the total (time-averaged) and peak SBS. As the electron temperature reaches 2.5 keV (solid blue, right axis), the total backscatter goes to zero. This corresponds to a gain of $g_{SBS} < 15$

with a respective resolution of 0.5 nm and 0.05 nm? .

The Near Backscatter Imager (NBI) measures the light outside of the original beam cone reflecting from an aluminum plate surrounding the interaction beam. The plate is imaged onto two charge-coupled devices (CCD) which time integrate the SBS and SRS signals. The cameras have been calibrated at 353 nm and 532 nm with a pulsed calibration laser of known energy that is reflected by the plate at various locations. These backscattering diagnostics (FABS and NBI) allow us to measure the total reflected light with an accuracy of ~ 20 %. By correlating the plasma parameters, backscatter, and transmission measurements we are able to obtain a detailed scaling of laser scattering as a function of electron density and temperature.

RESULTS AND DISCUSSION

Outer Beam Plasma Emulator Results

Figure 3 shows a strong reduction in the backscattered light as the electron temperature along the hohlraum axis exceeds 2.5 keV for an interaction beam intensity of $I_p = 1.7 \times 10^{15}$ W cm^{-2}. The decrease in reflectivity with increasing temperature is a direct result of reducing the SBS three wave coupling as evident in the linear gain,

$$G_{sbs} = 1 \times 10^{-27} \left(\frac{Z n_e [\text{cm}^{-3}] L[\mu m]}{T_e[eV]} \right) \left(\frac{\omega_a}{\nu_a} \right) I[\text{W-cm}^{-3}] \tag{2}$$

where $n_e = 5 \times 10^{20}$ cm^{-3} is the electron density, Z=2.2 is the average charge state for our fully ionized CH gas and $L \sim 1600$ μm is the gain length. T_e/T_i changes by

less than 15% and the Landau damping for our conditions is $\nu_a/\omega_a \approx 0.1$. The theoretical curve in Fig. 3(a) is obtained by applying linear theory including pump depletion [13] ,

$$R(1-R) = \epsilon e^{G_o \frac{T_o}{T_e}(1-R)} \tag{3}$$

where $\epsilon \approx 10^{-9}$ is the thermal noise. The peak linear SBS gain calculated by post processing the plasma properties from HYDRA simulations using the code LIP[14] is $G_o = 24$ for $T_o = 1.8$ keV. At this intensity ($I_p = 1.7 \times 10^{15}$ W cm^{-2}), < 1 % backscattered light was detected by the NBI outside of the original beam cone. No SRS is measured in these experiments, as predicted by the moderate linear SRS gains ($G_{SRS} < 20$).

The SBS spectra measured by FABS (Fig. 4a) for a power averaged intensity in the interaction beam of $I_p = 1.7 \times 10^{15}$ W-cm^{-2} shows a narrow feature that peaks when the interaction beam reaches maximum power and the plasma is cold ($T_e = 1.8$ keV). The temporal reflectivity and wavelength shift of this spectra are well reproduced by the linear gain calculations shown in Fig. 4b where the SBS power spectrum has been calculated using linear theory, Eq. 3. The simulated reflectivity is consistent with the measurements when the instrument function ($\sigma = 100$ ps) has been convolved to account for the time shear introduced by the spectrometer. Both the simulation and the experimental results show that when the plasma reaches a temperature above 2.5 keV, the total backscatter is less than 1%.

Furthermore, the simulated SBS frequency shift is consistent with the measured spectrum when accounting for the frequency change observed in the forward scattered light [15]. The frequency of the light propagating in the plasma is shifted as it moves through the changing density. This is observed by the TBD as the transmitted light is shifted by a few Angstroms (Fig. 4) over the time of the experiment.

Low backscatter and high electron temperature leads to a peak transmission (Figure 5) greater than 90% for intensities $I_p \leq 2 \times 10^{15}$ W cm^{-2}. The total scattered power (TBD + backscatter) compares with well with HYDRA simulations that account for inverse bremsstrahlung absorption. The agreement between the measurements and calculations further indicates the lack of side scattering losses.

In addition to this high transmission, Fig. 6(b) shows that 75% of the total transmitted power is measured within the original ($f/6.7$) beam cone after propagation through the high temperature plasma. For intensities above $I_p > 2.0 \times 10^{15}$ W-cm^{-2}, transmission within twice the beam cone drops to 55% and 65% of the energy is outside of the original beam cone. Furthermore, backscattered light outside of the FABS is measured by the NBI. For the highest intensity shots (4×10^{15} W-cm^{-2}), 50% of the total backscattered energy is outside of the original beam cone.
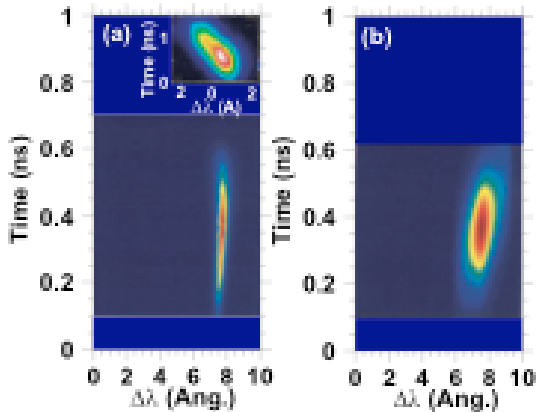
FIG. 4: (a) The narrow SBS spectra for a laser beam intensity of 1.7×10^{15} W-cm^{-2} indicates scattering from a uniform plasma created with a total heater beam energy of 16 kJ. At peak electron temperature ($T_e = 3.5$ keV), there is no measured SBS. Early in time, the plasma is cold ($T_e < 2$ keV) and a peak reflectivity of 25% is measured. The forward spectra is measured (insert) and shows a strong frequency shift in time. (b) The reflectivity is calculated using linear gains, Eq. 3. The wavelength shift early in time ($\Delta\lambda = 7.5$Å) is consistent with the simulated plasma parameters.

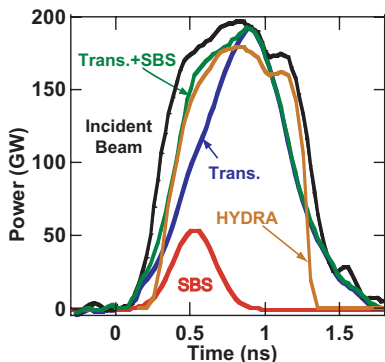FIG. 5: At peak electron temperature (t=800 ps), we measure a peak transmission above 90% (blue curve) for an interaction beam intensity of $I_p = 1.4 \times 10^{15}$ W cm^{-2}. The calculated transmission (orange curve) is determined by multiplying the absorption calculated by HYDRA with the incident laser pulse; these results compared to the total measured light in the interaction beam; the total measured light is equal to the sum of the measured transmission and the reflected light (red).

Beam spray is a direct measure of filamentation; the filamentation threshold for an ideal beam can be calculated by balancing the plasma pressure with the pondermotive force resulting from the transverse profile of the laser beam [16]. Theoretical work using the laser-plasma interaction code Pf3D has extended this work to include the laser beam intensity profile with a random
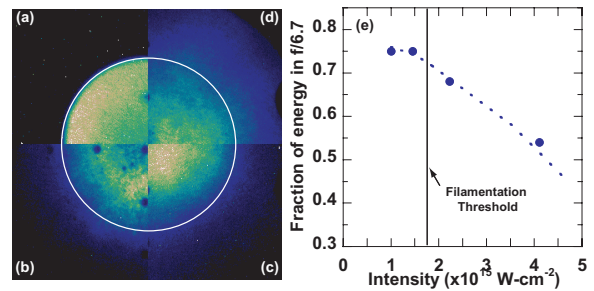

FIG. 6: The time integrated transmitted beam profile is a measure of the beam spray which is a direct indication of filamentation in the plasma; the incident intensity is varied (a) no plasma, (b) $I_p = 1.2 \times 10^{15}$W-cm^{-2}, (c) $I_p = 2 \times 10^{15}$W-cm^{-2}, (d) $I_p = 3.5 \times 10^{15}$W-cm^{-2}. (e) For intensities less than $I_{FFOM} = 1.5 \times 10^{15}$W-cm^{-2}, 70% of the energy is measured to remain in the original $f/6.7$ beam cone (circle).

phase plate (RPP) [17],

$$FFOM = \frac{I_p \lambda^2}{10^{13}} \left(\frac{n_e}{n_{cr}} \right) \left(\frac{3}{T_e} \right) \left(\frac{f^\#}{8} \right)^2 \qquad (4)$$

where I_p is the power averaged intensity at best focus, λ is the wavelength of the laser beam, $n_e/n_{cr} = 6\%$ is the fraction of electron density to the critical density at 3ω, $T_e = 3$ keV is the electron temperature, and $f^\# = 6.7$ is the ratio of the focal length to the beam diameter. When the filamentation figure of merit (FFOM) is greater than one, the beam is expected to experience significant filamentation and beam spray. Our measurements presented in Fig. 6(b) are compared with the peak FFOM determined by post-processing the parameters calculated by the hydrodynamic simulations where the filamentation threshold is calculated to be at $I_{FFOM} = 1.5 \times 10^{15}$ W-cm^{-2}; at intensities less than this threshold, there is good laser beam propagation through the plasma.

Inner Beam Plasma Emulator Results

Laser-plasma interaction experiments in hohlraums filled with higher gas densities have been performed at Omega to emulate the plasma conditions encountered by the inner laser beam when they approach the dense capsule blow-off plasma in an ignition hohlraum. These experiments employ fill gas densities yielding electron densities of $n_e/n_{crit} = 0.11$ and electron temperatures of $T_e \approx 3$ keV at a scale length of 1.6 mm. These conditions are particularly relevant for 1.8 MJ ignition designs. On the other hand, recent ignition hohlraum calculations for 1 MJ laser energy indicate possibly even higher densities (up to $n_e/n_{crit} = 0.15$) and lower temperatures ($T_e = 2.5$ keV) in a shorter part of the laser beam path of $\sim 500\mu$m. Presently, these shorter scale length condi-
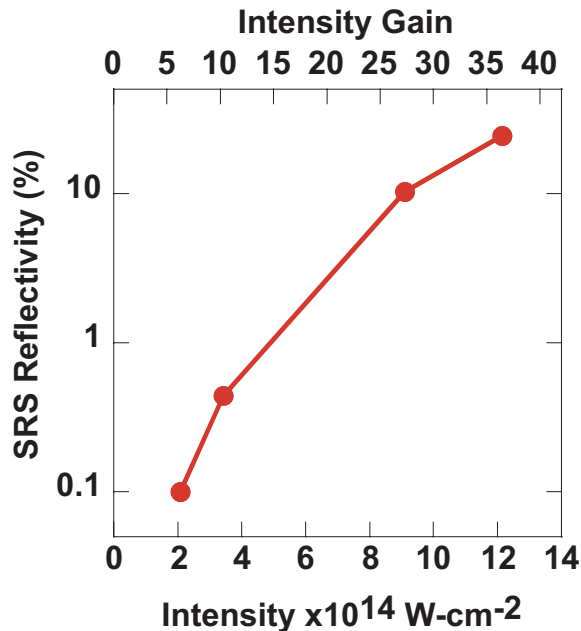
FIG. 7: The time integrated transmitted beam profile is a measure of the beam spray which is a direct indication of filamentation in the plasma; the incident intensity is varied (a) no plasma, (b) $I_p = 1.2 \times 10^{15}$W-cm^{-2}, (c) $I_p = 2 \times 10^{15}$W-cm^{-2}, (d) $I_p = 3.5 \times 10^{15}$W-cm^{-2}. (e) For intensities less than $I_{FFOM} = 1.5 \times 10^{15}$W-cm^{-2}, 70% of the energy is measured to remain in the original $f/6.7$ beam cone (circle).

tions have not been investigated at Omega and will be the focus of future work.

At high electron densities, we find that SRS is the dominant backscatter process. Figure 7 shows a strong dependency of the SRS backscattered light on the interaction beam intensity. The SRS reflectivity is reduced from > 10 % to < 1 % when reducing the intensity from $I_p = 1.2 \times 10^{15}$ W-cm^{-2} to $I_p = 2 \times 10^{14}$ W-cm^{-2}. In particular, for $I_p < 5 \times 10^{14}$ W-cm^{-2} we find that SRS is negligible, < 1 % while SBS is < 5 %. As it was found for SBS, this decrease of the SRS reflectivity with decreasing intensity can be explain by a reduction of the SRS three wave coupling as evident in the linear gain. We find that gain values < 25 are required to obtain small scattering losses in these conditions. Besides accessing higher density shorter scale conditions, future work is intended to provide a better estimate of the maximum possible gain in this regime by performing experiments with intensities of $I_p = (6 - 8)) \times 10^{14}$ W-cm^{-2}. These data will be important because present designs of the inner beam focal spot indicate intensities in this regime.

SUMMARY AND OUTLOOK

In summary, we have demonstrated laser beam propagation through ICF hohlraums at ignition plasma con-ditions. This is accomplished through high electron temperature plasmas that reduce the linear gains below their thresholds ($G_{SBS,SRS} < 20$, FFOM< 1). For electron temperatures above 3 keV total backscatter is shown to be below 1% for outer ignition laser beam conditions while producing a transparent plasma with a peak transmission greater than 90%. The laser beam is shown to propagate without beam spray for intensities below 2×10^{15} W-cm^{-2}; above this intensity the beam is shown to filament.

For inner ignition hohlraum laser beam conditions, the relevant laser beam intensities are smaller than for outer beam conditions, electron densities are larger and temperatures are smaller resulting in scattering levels that are strongly increasing with the laser beam intensity. For present ignition designs, the intensity is to remain at $< 8 \times 10^{14}$ W-cm^{-2}. This will be accomplished by choosing the appropriate laser spot and by absorption before the beam interacts with the higher density capsule blow-off plasma. In these conditions, the present experiments indicate that scattering levels < 5 % may be achieved.

The present experiments verify the ability of current models to predict ignition hohlraum conditions and laser-plasma interaction linear gains for filamentation, SBS, and SRS. Furthermore, these results show the importance of predicting the electron temperature prior to peak power when the plasma is cold; a small change in the electron temperature can lead to a significant increase in the backscattered energy. These issue will be addressed in future experiments where we plan to continue scattering measurements in high-electron temperature targets under a wide range of densities, materials, and laser smoothing conditions.

[*] Electronic address: froula1@llnl.gov
[†] Also at UCSD
[1] J. D. Lindl *et al.*, Phys. Plasmas **11**, 339 (2004).
[2] W. L. Kruer, *The Physics of laser plasma interactions* (Addison-Wesley Publishing Company, Inc., 1988).

[3] D. H. Froula *et al.*, Phys. Plasmas **13** (2006).

[4] J. M. Soures *et al.*, Laser Particle Beams **11**, 317 (1993).

[5] M. M. Marinak *et al.*, Phys. Plasmas **8**, 2275 (2001).

[6] S. H. Glenzer *et al.*, Phys. Plasmas **6**, 2117 (1999).

[7] A. J. MacKinnon *et al.*, Rev. Sci. Instrum. **75**, 3906 (2004).

[8] D. H. Froula *et al.*, Rev. Sci. Instrum. **In press** (2006).

[9] B. MacGowan *et al.*, Phys. Plasmas **3**, 2029 (1996).

[10] J. Moody *et al.*, Phys. Plasmas **7**, 3388 (2000).

[11] J. C. Fernandez *et al.*, Phys. Rev. Lett. **81**, 2252 (1998).

[12] B. H. Failor *et al.*, Physical Review E **59**, 6053 (1999).

[13] C. Tank, J. Appl. Phys. **37**, 2945 (1966).

[14] E. A. Williams, Report UCRL-LR-105820-98 (1998).

[15] T. DEWANDRE *et al.*, Phys. Fluids **24**, 528 (1981).

[16] P. KAW *et al.*, Phys. Fluids **16**, 1522 (1973).

[17] E. A. Williams, Phys. Plasmas **13**, 056310 (2006).